A Comparative Study on the Diastereofacial Control in the [4+2] Cycloaddition of Sorbates and the Ene Reaction of Tiglates with Singlet Oxygen and PTAD by a Variety of Chiral Auxiliaries

Waldemar Adam,*[a] Sara G. Bosio,[a] Hans-Georg Degen,[a] Oliver Krebs,[a] Dietmar Stalke,[b] and Dirk Schumacher[a]

Keywords: Peroxides / Cycloaddition / Ene reaction / Singlet oxygen

The auxiliary-induced diastereoselectivities of [4+2] cycloaddition and the ene reaction of singlet oxygen and PTAD through a variety of auxiliaries is studied. The different trends in the diastereoselectivities that are observed for the diverse auxiliaries, which include 2,2-dimethyloxazolidines, a menthol derivative, several related cyclohexanes, and the Oppolzer sultam, are compared and backed by mechanistic interpretations. From this overview of two reaction modes for two electrophiles and four different types of auxiliaries, the advantages of the individual auxiliaries become evident and comprehensible.

Introduction

The auxiliary-controlled diastereoselective [4+2] cycloaddition and ene reaction of singlet oxygen, the smallest possible enophile, and the larger PTAD (4-phenyl-1,2,4-triazoline-3,5-dione) have received much attention in the last few years.[1−5] Although the diastereoselectivities of the ene reaction and of the [4+2] cycloaddition with singlet oxygen were greatly improved[1,3,5] since the first efforts,[6,7] little preparative use has been made of this. This may be in part due to the drastic conditions that are needed to release the auxiliaries through hydrolysis.[8,9]

With the optically active 2,2-dimethyloxazolidines **A** and **B** as auxiliaries, diastereoselectivities of up to 95:5 (Table 1, Entries 1 and 2) have been obtained for the [4+2] cycloaddition of the sorbic amides **2A** and **2B**, both with singlet oxygen and PTAD.[1] However, in the singlet-oxygen ene reaction of the tiglic amides **1A** and **1B**,[2] these auxiliaries failed to control the diastereoselectivity for $^1O_2$ (Entries 1 and 2), but were successful for the larger PTAD (*dr* ≥ 95:5, Table 1, Entries 1 and 2).

The menthol-derived auxiliary **C** resulted in a better diastereoselectivity (up to 82:18) for the singlet-oxygen ene reaction of the tiglate **1C** (Entry 3). Thus, for the auxiliary **C**, diastereofacial control was expected also in the [4+2] cycloaddition of singlet oxygen with such sorbates. Moreover, the hydrolysis of an ester functionality should be achieved under milder conditions than that of an amide.

Table 1. Diastereoselectivities in the [4+2] cycloaddition with sorbic acid derivatives, and in the ene reaction with tiglic acid derivatives

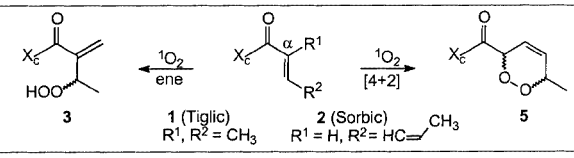

Entry	dr[a] $^1O_2$	dr[a] PTAD	π-Facial attack	X_c	dr[b] $^1O_2$	dr[b] PTAD	π-Facial attack
1	50:50	≥ 95:5	α-*Re*	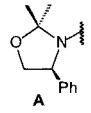 A	90:10	≥ 95:5	α-*Si*
2	60:40	≥ 95:5	α-*Re*	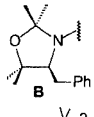 B	≥ 95:5	–	α-*Si*
3	70:30[c] 82:18[d]	–	α-*Re*	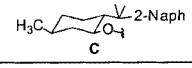 C	–	–	–

[a] Ref.[2] [b] Ref.[1] [c] At 25 °C, Ref.[5] [d] At −60 °C, Ref.[5]

[a] Institut für Organische Chemie, Universität Würzburg, Am Hubland, 97074 Würzburg, Germany
Fax: (internat.) + 49-(0)931/888-4756
E-mail: adam@chemie.uni-wuerzburg.de
http://www-organik.chemie.uni-wuerzburg.de/ak adam/
[b] Institut für Anorganische Chemie, Universität Würzburg, Am Hubland, 97074 Würzburg, Germany

Since d'Angelo and Dumas[10,11] have shown that the cyclohexane-based auxiliaries **D**−**F** are equally efficient as the menthol-derived auxiliary **C** in controlling the stereoselectivity, the racemic sorbates **2D**−**F** (Scheme 1) were chosen to test their potential for diastereofacial differentiation in the [4+2] cycloaddition with singlet oxygen and PTAD. Moreover, since auxiliary **C** in the tiglate **1C** is more effective in steering the ene reaction with singlet oxygen than the amides **1A** and **1B**, the more readily prepared racemic esters **2G** and **2H** were also selected.

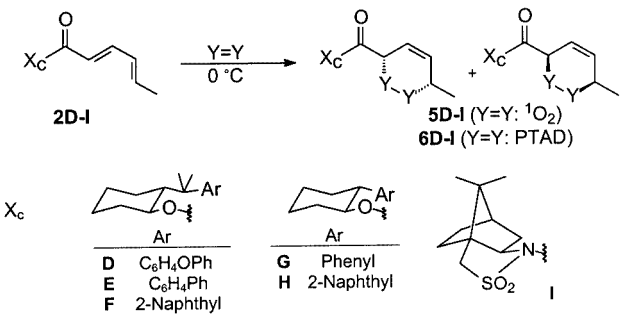

Scheme 1. [4+2] cycloaddition of $^1O_2$ and PTAD to sorbates **2D**−**I**, derivatized with chiral auxiliaries **D**−**I**

The sultam **I** operates on the basis of electrostatic rather than steric interactions.[12,13] To test the efficacy of this concept in controlling the diastereoselectivity of the [4+2] cycloaddition and of the ene reaction with $^1O_2$ and PTAD, the sorbic and tiglic fragments were linked to the sultam auxiliary.

This comparative study encompasses a comprehensive survey of the auxiliary-induced diastereoselectivities for ene reactions and [4+2] cycloadditions of PTAD and singlet oxygen of alkenoates and dienes tethered to four different classes of chiral auxiliaries, namely oxazolidines, a menthol derivative, several related cyclohexanes, and the Oppolzer sultam. The results provide the first comprehensive mechanistic overview on the advantages as well as disadvantages that these auxiliaries exercise in the stereochemical control of the pericyclic reactions under scrutiny.

Results

The auxiliaries **D**−**I** were prepared according to literature procedures,[10] and the esters **2D**−**H** in analogy to the method described by Dussault[5] (see Exp. Sect.). The amides **1I** and **2I** have been previously reported.[14,15]

The results of the cycloaddition of $^1O_2$ and PTAD with the sorbic acid derivatives **2** are summarized in Table 2. The cycloadditions for both dienophiles were conducted at 0 °C. The photo-oxygenations required 16 h in CCl_4, while cycloadditions with PTAD took only 10 min in dichloromethane. For both dienophiles, the [4+2] cycloadducts were the only detectable products after complete consumption of the starting materials.

Table 2. Diastereoselectivities for the [4+2] cycloaddition of $^1O_2$ and PTAD with sorbates **2D**−**H**, functionalized with chiral auxiliaries **D**−**H**

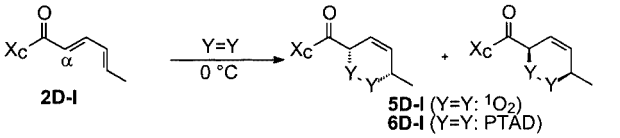

Entry	Chiral auxiliary X_c	Substrate	Ar	dr[a] $^1O_2$[b]	dr[a] PTAD[c]	π-Facial attack
1		**2D**	C_6H_4OPh	68:32	74:26	α-*Si*
2	**D**–**F**	**2E**	C_6H_4Ph	64:36	69:31	α-*Si*
3		**2F**	2-Naph	69:31	78:22 82:18[d] 85:15[e]	α-*Si*
4		**2G**	Ph	54:46	67:33	α-*Si*
5	**G**, **H**	**2H**	2-Naph	60:40	68:32	α-*Si*

[a] Determined from characteristic signals of the ^1H NMR spectra; error ca. 5% of the stated value. [b] 16 h in CCl_4. [c] 10 min in CH_2Cl_2. [d] 2 d at −45 °C. [e] 2 d at −58 °C.

The diastereoselectivities for the [4+2] cycloaddition of esters **2D**−**F** with singlet oxygen were all below 70:30 (Table 2, Entries 1−3); however, also for the larger PTAD, the diastereoselectivity was only marginally higher (Entries 1−3). For example, with the naphthyl-substituted auxiliary **F**, the highest *dr* value of 78:22 was observed within this series of substrates, which was increased only to 82:18 at −45 °C, and to 85:15 even at −58 °C. This enhancement in the diastereoselectivity is just barely outside the error limit of analysis (ca. ±5% of the stated values).

Even lower diastereoselectivities were obtained in the photo-oxygenation of esters **2G**−**H**, the *dr* values were only 60:40 and below. The [4+2] cycloaddition with PTAD resulted in diastereoselectivities of merely 68:32 (Table 2, Entries 4 and 5).

The optically active amide **2I** afforded the highest diastereoselectivities in this study. Thus, the photo-oxygenation gave the two possible diastereomers of the endoperoxide **5I** in a 75:25 ratio (Scheme 2), whereas the PTAD cycloaddition yielded the adduct **6I** in as high a *dr* value as 94:6 (Scheme 2). In view of these encouraging results, the ene reaction of tiglic amide **1I** was examined.[16] The photo-oxygenation of **1I** at 0 °C led to the diastereomeric hydroperoxides **3I** in a ratio of 83:17 (Scheme 2).

The configurations of the [4+2] cycloaddition adducts were determined by X-ray analysis of the PTAD derivatives. Representative of esters **2D**−**F**, the crystal structure of the PTAD cycloadduct **6F** shows that the [4+2] cycloaddition of the racemic (1*S**,2*R**)-ester **2F** gave principally the (1*S**,2*R**,5*S**,8*S**) diastereomer through α-*Si* face[17] attack (Figure 1). Also for esters **2G** and **H**, the [4+2] cycloaddition from the α-*Si* face was preferred, so that racemic (1*R**,

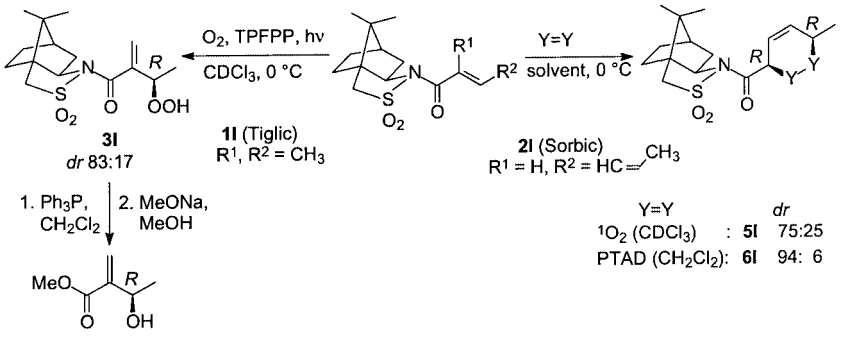

Scheme 2. Ene reaction of optically active tiglic amide **1I** with $^1O_2$ and [4+2] cycloaddition of sorbic amide **2I** with $^1O_2$ and PTAD

2*S**)-sorbate **2H** produced preferably the (1*R**,2*S**,5*R**,8*R**)-PTAD adduct **6H** (Figure 1). Reaction of the optically active amide **2I** with auxiliary **I** gave preferentially the (−)-(6*R*,3a*S*,7a*R*,5*R*,8*R*)-PTAD cycloadduct **6I** through α-*Re* face attack, as shown by the crystal structure of the minor (6*R*,3a*S*,7a*R*,5*S*,8*S*) diastereomer (Figure 1).

To assess the stereochemical course for the ene reaction with singlet oxygen, hydroperoxide **3I** was submitted to reduction and subsequent methanolysis to afford the known[18] (−)-(*R*)-hydroxy alcohol (Scheme 2).[16] This chemical correlation establishes that hydroperoxide **3I** possesses the (*R*) configuration at the newly generated chirality center and, thus, the photo-oxygenation proceeds predominantly from the α-*Si* face.

To answer the question of whether π stacking is operative in the reactions of the sorbic esters with the chiral auxiliaries **D**−**H**, low-temperature NMR experiments were conducted on sorbate **2F** as representative case. The results in Table 3 show a significant upfield shift of the β-H atom in ester **2F** (Table 3, bottom Entry). Thus, at room temperature, the β-H atom shows a proton resonance at δ = 6.44 ppm, while at −50 °C it is shifted by 0.32 ppm to δ = 6.12 ppm, which implicates π stacking. Similar low-temperature NMR shifts were observed by Dussault[5] for tiglate **1C** (Table 3, upper Entry), which was interpreted in terms of greater aryl-induced shielding for the *s-trans* conformer, the major isomer at low temperature.

Discussion

The observed diastereoselectivities for the [4+2] cycloaddition of singlet oxygen and PTAD with sorbic derivatives **2D**−**I** (Table 2 and Scheme 2) convey a number of unexpected results that need to be interpreted mechanistically. For the diastereoselectivities of the cyclohexane-type auxiliaries **C**−**F**, it was found that the [4+2] cycloaddition of PTAD and singlet oxygen with sorbic esters **2D**−**F** (Table 2, Entries 1−3) took place from the opposite π face (α-*Si*) than was observed for the singlet-oxygen ene reaction with tiglate **1C** (Table 1, Entry 3), which attacked from the α-*Re* face.[5]

A comparison of the cyclohexane-type auxiliaries **C**−**F** with the oxazolidine-type auxiliaries **A** and **B** reveals an opposing trend for the two types of auxiliaries in the diastereoselectivities of the [4+2] cycloaddition (Table 1, Entries 1 and 2; Table 2, Entries 1−3) and ene reaction (Table 1, left column) of singlet oxygen: While for the oxazolidine-type auxiliaries **A** and **B** (Table 1, Entries 1 and 2), the [4+2] cycloaddition of singlet oxygen with sorbic amides **2A** and **2B** is much more selective than their ene reaction with tiglic amides **1A** and **1B**, for the cyclohexane-type auxiliaries **C**−**F** the opposite applies, that is, the [4+2] cycloaddition with sorbates **2D**−**F** (Table 2, Entries 1−3) is less selective than the ene reaction with tiglate **1C** (Table 1, Entry 3). To rationalize these results mechanistically, an in-depth survey of the structural differences of these chiral auxiliaries shall now be made, with particular emphasis on the stereochemically controlling features.

For the oxazolidine-type auxiliaries **A** and **B**, the diastereofacial preference in the [4+2] cycloaddition arises from conformational control and simultaneous steric shielding (Structure **2A**).[19] The carbonyl oxygen atom is locked between the two methyl groups on the C-2 carbon atom (*syn* arrangement). Therefore, the R substituent on the oxazolidine ring constrains the dienoate to the s-*cis* and s-*trans* conformer, and blocks the α-*Re* approach of the incoming dienophile to the s-*cis* conformer of the diene.

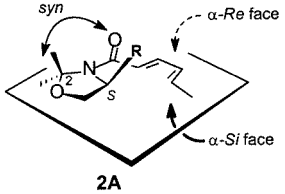

2A

In the case of tiglic amides **1A** and **1B**, efficient diastereofacial control for the ene reaction is exercised only for the sterically more demanding PTAD, not for the small singlet oxygen (Table 1, Entries 1 and 2). As a rationale, we have previously proposed that a coplanar conformation in the tiglic amides **1A** and **1B** is not accessible due to steric interactions between the carbonyl functionality and the α-methyl group on the C=C double bond.[2,20] Thus, the tiglic

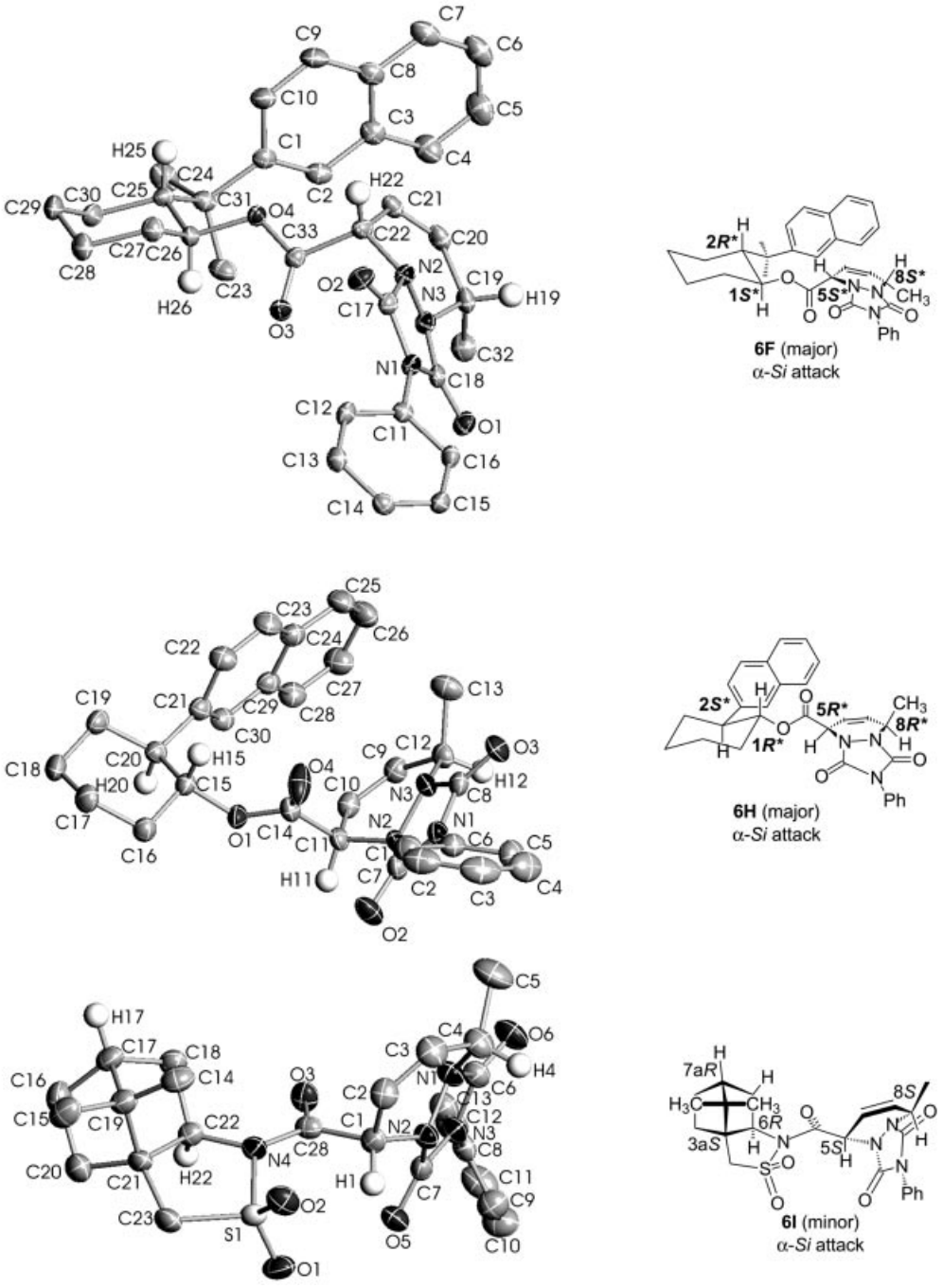

Figure 1. Crystal structures of the major isomer **6F**, the major isomer **6H**, and the minor isomer **6I** with their configurations

functionality assumes either of the two twisted conformers in Scheme 3. In the transition state **1A**$^{\neq}$ for the enophilic attack (α-*Re* face), the steric interactions are less severe, since the original β-methyl group at the incipient stereogenic sp^3-hybridized carbon atom points away from the sterically imposing phenyl group of the oxazolidine-type auxiliary. In the case of singlet oxygen, however, the steric shielding does not suffice to repel this small and sterically undemanding enophile from the shielded face. Thus, for the tiglates derived from the oxazolidine-type auxiliaries **A** and **B**, the presence of an α-methyl group precludes a planar enone subunit, which prevents efficient diastereofacial discrimination in the singlet oxygen ene reaction.

For tiglate **1C**, the π-facial control in the ene reaction with $^1O_2$ has been previously rationalized as a result of effective steric shielding by the naphthyl ring in the s-*trans* conformer.[5] At low temperature, the more stable s-*trans* conformer is preferentially populated, as confirmed by low-temperature ^{1}H NMR experiments (Table 3, upper Entry) and, consequently, a moderate increase in the *dr* value from 70:30 at 25 °C to 82:18 at −60 °C (Table 1, Entry 3) was observed.[5] To rationalize the observed diastereoselectivi-

Table 3. Low-temperature ^{1}H NMR spectroscopic data for the β-H atom in tiglate **1C** and sorbate **2F**

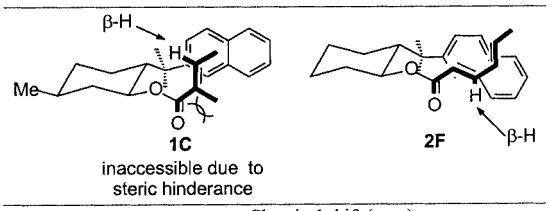

Substrate	T [°C]	Chemical shift (ppm) r.t.[a]	–20	–40	–50	–60
Tiglate **1C**[b]		5.77	5.41	5.30	–	5.18
Sorbate **2F**[c]		6.44	6.25	–	6.12	–

[a] Room temperature was 20 °C for the sorbate and 25 °C for the tiglate. [b] Ref.[5] [c] Measured at 200 MHz.

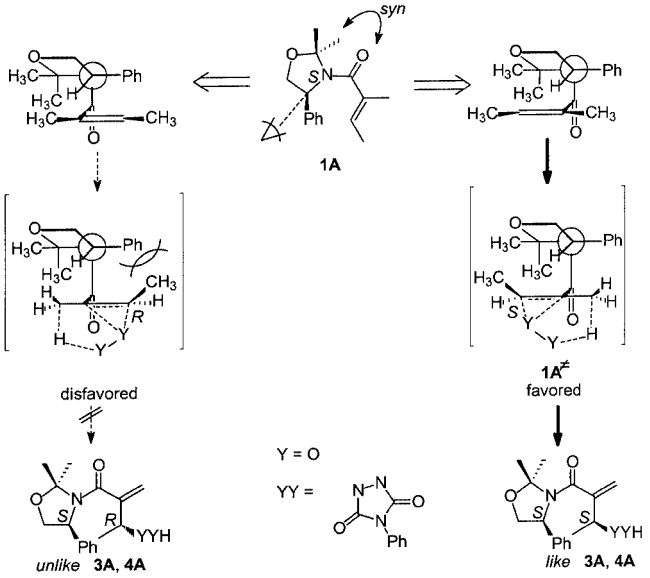

Scheme 3. Transition structures for the ene reaction of tiglic amide **1A**

ties of this ene reaction, it was argued that singlet oxygen attacks from the α-*Re* face of the s-*trans* conformer, which is not shielded by the naphthyl ring of the cyclohexane-type auxiliary **C**, as depicted in the structure of substrate **1C** (Table 3). However, in view of more recent reports, a twisted conformer is more likely in tiglates than a coplanar one,[2,20] and the ene reaction should take place from such a twisted s-*trans* conformer. Although conjugation between the C=C double bond and the carbonyl group should be minimal in the twisted enone conformer, the C=C double bond is presumably still sufficiently electron-poor due to the inductive effect of the carbonyl group to be receptive for π stacking, as experimentally manifested (Table 3, upper Entry).

In sorbates **2D**−**F**, there is no α-methyl substituent and, thus, no steric impediment in populating the coplanar conformers. The low-temperature ^{1}H NMR shift of the β-H atom (Table 3, lower Entry) conveys effective π stacking between the sorbic fragment and the naphthalene ring, which has been reported to take place preferably in the s-*trans* conformer.[5,10] Nevertheless, the [4+2] cycloaddition occurs on the α-*Si* face of the enone, which corresponds to an attack on the s-*cis* conformer. Moreover, at low temperatures, where π stacking is more effective in the sorbate derivative **2F** (Table 3, lower Entry), no significant increase in the *dr* value was observed (Table 2, Entry 3). Thus, it may be concluded that π stacking, although present, does not play a decisive role in the stereochemical course of the [4+2] cycloaddition with sorbate **2F**. In fact, the small energy difference between the s-*cis* and s-*trans* conformers, recently documented for the crotic derivatives of auxiliary **F**,[21] also applies for the sorbates and diastereofacial control is ineffective. This conclusion is also supported by the fact that the diastereoselectivities in the [4+2] cycloaddition for sorbates **2G** and **2H** (up to 74:26) are only marginally lower than those for sorbates **2D**−**F** (up to 78:22 at 0 °C). For sorbates **2G** and **2H**, the widening V arrangement[5] (Figure 2) does not allow π stacking and, expectedly, purely steric interactions control the diastereoselectivity. This is also corroborated by comparing the signals of the vinylic protons in the NMR spectrum of **2H**, which are shifted to lower field with respect to **2F** (see Exp. Sect.).

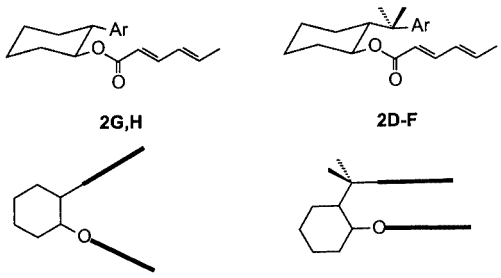

Figure 2. Schematic geometrical arrangement of the chiral auxiliaries **G**, **H** and **D**−**F** in the sorbates **2**

For the auxiliary **I**, the relevant conformations are not controlled by steric interactions, but by electrostatic repulsion. These occur between the sulfonyl and the carbonyl group of the amide functionality, as well as with the incoming dienophile or enophile.[12,13,20] For tiglic amide **1I**, the preferred orientation of the tiglic fragment is known from its X-ray structure,[15] in which the carbonyl group points away from the sulfonyl functionality and the s-*trans* conformer prevails to avoid interactions between the sulfonyl functionality and the α-methyl group. As in the literature cases,[20] the attack takes place from the upper (α-*Si*) side, which is less shielded by the sulfonyl group than the lower (α-*Re*) face. By analogy, the same applies for sorbic amide **2I**: The cycloaddition occurs preferably from the upper side, since the negatively polarized oxygen atoms of the sulfonyl functionality are located on the lower face. In contrast to the tiglic amide **1I**, the s-*cis* conformation is preferred for sorbic amide **2I**; the upper side is now the α-*Re* face, from which [4+2] cycloaddition occurs (Structures **1I** and **2I**). This is in agreement with reports on the [3+2] cycloaddition of nitrile oxides[12] and silyl nitronates[13] for the crotic derivative of auxiliary **I**.[15] Thus, the extent of the diastere-

ofacial differentiation for the ene and [4+2] cycloaddition reaction modes is comparable only for auxiliary **I**, which relies on electrostatic interactions, both for the control of conformations and the direction of the attack by $^1O_2$ and PTAD.

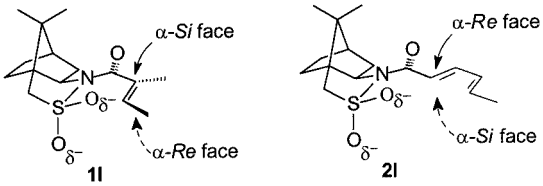

In summary, we have shown that the sense and the extent of diastereofacial control for various chiral auxiliaries depends on conformational effects and the steric as well as electrostatic interactions of the substrate with the auxiliary. The coplanar arrangement of the enone functionality is essential for a diastereoselective attack of singlet oxygen in the case of oxazolidine auxiliaries **A** and **B**. For the sorbates **2A** and **2B**, the coplanar conformer is accessible and provides high diastereoselectivities, but for tiglates **1A** and **1B**, the twisted conformation of the enone functionality prevents efficient diastereofacial control in the ene reaction of singlet oxygen. For the cyclohexane-type auxiliaries **C**−**F**, the opposite applies: Both s-*trans* and s-*cis* coplanar arrangements of sorbates **2D**−**F** engage in effective π stacking and, consequently, only little diastereofacial control results. For tiglate **1C**, π-facial discrimination in the ene reaction of singlet oxygen is enhanced by π stacking, which favors the s-*trans* conformer. Although the sorbic amide **2I** and tiglic amide **1I** react through two different conformers, the electrostatic interactions of the sulfonyl functionality with the incoming reagent provide a similar level of diastereoselection.

Experimental Section

General: Sorbinyl chloride[14], the auxiliaries **D**−**H**,[11] 4-phenyl-1,2,4-triazoline-3,5-dione (PTAD)[22], (1*S*,2*R*)-bornane-10,2-sultam[23] [from (1*S*)-(+)-camphorsulfonic chloride], and *N*-[(*E*,*E*)-2,4-hexadienoyl]bornane-10,2-sultam[14] were prepared according to literature procedures. The ^1H and ^{13}C NMR spectra were recorded with a Bruker AC200 (^1H: 200 MHz, ^{13}C: 50 MHz), a Bruker AVANCE 400 (^1H: 400 MHz, ^{13}C: 100 MHz) or on a Bruker DMX 600 (^1H: 600 MHz, ^{13}C: 150 MHz) spectrophotometer. The diastereomeric ratios were determined from the ^1H NMR spectra of the crude product mixtures, and the multiplicities of the ^{13}C signals were assigned by CH correlation. The IR spectra were measured with a Perkin−Elmer 1600 FT-IR spectrophotometer. Solvents and commercially available chemicals were purified by standard procedures. PE = petroleum ether.

Representative Procedure for 2-[1-Methyl-1-(4-phenoxyphenyl)ethyl-]cyclohexyl (2*E*,4*E*)-2,4-Hexadienoate (2D): To a stirred solution of 2-[1-methyl-1-(4-phenoxyphenyl)ethyl]cyclohexanol (748 mg, 2.41 mmol) in dry THF (20 mL) under argon at 0 °C and ca. 2 mg of 1,10-phenanthroline as indicator, was added a 1.0 M solution of *n*-butyllithium (ca. 1 equiv.) until a dark red color indicated the complete deprotonation of the alcohol. After 15 min, sorbinyl chloride (345 mg, 2.35 mmol) was added and stirring was continued for 2 h. Removal of the solvent (30 °C, 20 mbar) followed by silica gel chromatography [PE/Et_2O (20:1)] and subsequent recrystallisation from hexane yielded 680 mg (70%) the ester as yellow needles, m.p. 109−110 °C. IR (KBr): $\tilde{\nu}$ [cm^{-1}] = 3255, 2924, 2854, 1699, 1645, 1620, 1329, 1245, 1189, 1142, 1000. ^1H NMR (400 MHz, $CDCl_3$): δ [ppm] = 1.03−1.40 (m, 4 H, CH_2), 1.22 (s, 3 H, CH_3), 1.31 (s, 3 H, CH_3), 1.63−1.76 (m, 3 H, CH_2), 1.85 (d, J = 4.8 Hz, 3 H, CH_3), 1.91−1.98 (m, 1 H, CH_2), 2.05 (dt, J = 3.0, 11.6 Hz, 1 H, CH), 4.83 (dt, J = 4.3, 10.4 Hz, 1 H, CH), 5.36 (d, J = 14.9 Hz, 1 H, CH), 6.03−6.14 (m, 2 H, CH), 6.87−6.96 (m, 3 H, CH and Ar-H), 6.99−7.02 (m, 2 H, Ar-H), 7.05−7.10 (m, 1 H, Ar-H), 7.20−7.25 (m, 2 H, Ar-H), 7.29−7.35 (m, 2 H, Ar-H).^{13}C NMR (100 MHz, $CDCl_3$): δ [ppm] = 18.6 (q), 24.7 (t), 25.6 (q), 26.0 (t), 27.2 (t), 27.7 (q), 33.4 (t), 39.6 (s), 51.2 (d), 74.5 (d), 118.3(d), 118.6 (d), 119.6 (d), 122.9 (d), 126.7 (d), 129.6 (d), 129.8 (d), 139.0 (d), 144.4 (d), 146.6 (s), 154.3 (s), 157.5 (s), 166.4 (s). $C_{27}H_{32}O_3$ (404.6): calcd. C 80.16, H 7.97; found C 79.83, H 7.51.

2-[1-Methyl-1-(4-phenylphenyl)ethyl]cyclohexyl (2*E*,4*E*)-2,4-Hexadienoate (2E): According to the method described for **2D**, the ester **2E** was obtained in 87% yield after silica gel chromatography [PE/Et_2O (20:1)] as a colorless powder, m.p. 82−83 °C. IR (KBr): $\tilde{\nu}$ [cm^{-1}] = 3252, 2974, 2920, 2854, 1706, 1651, 1624, 1594, 1549, 1384, 1371, 1238, 1005. ^1H NMR (400 MHz, $CDCl_3$): δ [ppm] = 1.07−1.38 (m, 4 H, CH_2) 1.25 (s, 3 H, CH_3), 1.35 (s, 3 H, CH_3), 1.66 (d, J = 4.9 Hz, 3 H, CH_3), 1.68−1.74 (m, 2 H, CH_2), 1.80−1.87 (m, 1 H, CH_2), 1.91−1.96 (m, 1 H, CH_2), 2.15 (m, 1 H, CH), 4.20−4.88 (m, 1 H, CH), 5.18 (d, J = 15.3 Hz, 1 H, CH), 5.83−5.94 (m, 2 H, CH), 6.71−6.78 (m, 1 H, CH), 7.28−7.36 (m, 3 H, Ar-H), 7.38−7.43 (m, 2 H, Ar-H), 7.48−7.51 (m, 2 H, Ar-H), 7.65−7.60 (m, 2 H, Ar-H). ^{13}C NMR (100 MHz, $CDCl_3$): δ [ppm] = 18.3 (q), 24.2 (q), 24.8 (t), 26.1 (t), 27.0 (t), 28.5 (q), 33.4 (t), 39.7 (s), 51.1 (d), 74.3 (d), 119.5 (d), 125.9 (d), 126.5 (d), 126.8 (d), 126.9 (d), 128.6 (d), 129.8 (d), 137.4 (s), 138.7 (d), 140.9 (s), 144.1 (d), 151.1 (s), 166.3 (s). $C_{27}H_{22}O_2$ (388.6): calcd. C 83.46, H 8.30; found C 83.23, H 8.21.

2-[1-Methyl-1-(2-naphthyl)ethyl]cyclohexyl (2*E*,4*E*)-2,4-Hexadienoate (2F): According to the method described for **2D**, the ester **2F** was obtained in 90% yield after silica gel chromatography [PE/Et_2O (20:1)] as a colorless powder, m.p. 66−67 °C. IR (KBr): $\tilde{\nu}$ [cm^{-1}] = 3027, 2979, 2858, 1700, 1645, 1598, 1501, 1445, 1389, 1197, 1084. ^1H NMR (600 MHz, $CDCl_3$): δ [ppm] = 1.10−1.36 (m, 6 H, CH_2), 1.29 (s, 3 H, CH_3), 1.41 (s, 3 H, CH_3), 1.70 (d, J = 4.9 Hz, 3 H, CH_3), 1.80−1.82 (m, 1 H, CH_2), 1.92−1.94 (m, 1 H, CH_2), 2.24 (dt, J = 11.9, 3.3 Hz, 1 H, CH), 4.88 (dt, J = 4.4, 10.3 Hz, 1 H, CH), 4.91 (d, J = 15.4 Hz, 1 H, CH), 5.58−5.65 (m, 2 H, CH), 6.43−6.48 (m, 1 H, CH), 7.35−7.39 (m, 2 H, Ar-H), 7.52 (dd, J = 8.7, 2.0 Hz, 1 H, Ar-H), 7.60 (br. s., 1 H, Ar-H), 7.71−7.72 (m, 1 H, Ar-H), 7.75−7.77 (m, 1 H, Ar-H), 7.56 (d, J = 8.7 Hz, 1 H, Ar-H). ^{13}C NMR (100 MHz, $CDCl_3$): δ [ppm] = 18.4 (q), 24.3 (q), 24.7 (t), 26.1 (t), 27.1 (t), 28.2 (q), 33.4 (t), 39.9 (s), 50.7 (d), 74.3 (d), 119.2 (d), 122.8 (d), 124.7 (d), 125.0 (d), 125.6 (d), 127.2 (d), 127.3 (d), 128.0 (d), 129.4 (d), 131.4 (s), 133.6 (s), 138.2 (d), 144.1 (d), 149.3 (s), 166.3 (s). $C_{25}H_{30}O_2$ (362.5): calcd. C 82.83, H 8.34; found C 83.05, H 8.29.

2-Phenylcyclohexyl (2*E*,4*E*)-2,4-Hexadienoate (2G): According to the method described for **2D**, the ester **2G** was obtained in 85% yield after silica-gel chromatography [PE/Et_2O (20:1)] as a colorless powder, m.p. 70−71 °C. IR (KBr): $\tilde{\nu}$ [cm^{-1}] = 3032, 2938, 2856, 1699, 1639, 1613, 1493, 1446, 1329, 1192, 1007. ^1H NMR

(400 MHz, $CDCl_3$): δ [ppm] = 1.26−1.64 (m, 4 H, CH_2), 1.75−1.90 (m, 3 H, CH_2), 1.80 (d, J = 5.4 Hz, 3 H, CH_2), 2.16−2.20 (m, 1 H, CH_2), 2.68−2.75 (m, 1 H, CH), 5.00−5.07 (m, 1 H, CH), 5.53 (d, J = 15.4 Hz, 1 H, CH), 5.98−6.10 (m, 2 H, CH), 6.99−7.05 (m, 1 H, CH), 7.13−7.27 (m, 5 H, Ar-H). ^{13}C NMR (100 MHz, $CDCl_3$): δ [ppm] = 18.5 (q), 24.8 (t), 25.9 (t), 32.4 (t), 34.0 (t), 49.7 (d), 75.7 (d), 119.2 (d), 126.3 (d), 127.4 (d), 128.2 (d), 129.8 (d), 138.7 (d), 143.2 (s), 144.4 (d), 166.6 (s). $C_{18}H_{22}O_2$ (270.4): calcd. C 79.96, H 8.20; found C 80.22, H 8.14.

2-(2-Naphthyl)cyclohexyl (2*E*,4*E*)-2,4-Hexadienoate (2H): According to the method described for **2D**, the ester **2H** was obtained in 90% yield after silica gel chromatography [PE/Et_2O (20:1)] as a white powder, m.p. 100−101 °C. IR (KBr): ṽ [cm^{-1}] = 3052, 3016, 2940, 2920, 1702, 1642, 1616, 1508, 1442, 1241, 1120. ^{1}H NMR (400 MHz, $CDCl_3$): δ [ppm] = 1.37−1.78 (m, 4 H, CH_2), 1.76 (d, J = 5.3 Hz, 3 H, CH_3), 1.80−1.94 (m, 2 H, CH_2), 1.98−2.06 (m, 1 H, CH_2), 2.22−2.28 (m, 1 H, CH_2), 2.88−2.95 (m, 1 H, CH), 5.18 (ddd, J = 10.5, 10.5, 4.4 Hz, 1 H, CH), 5.50 (d, J = 15.4 Hz, 1 H, CH), 5.92−6.04 (m, 2 H, CH), 6.96−7.03 (m, 1 H, CH), 7.37−7.45 (m, 3 H, Ar-H,), 7.66 (br. s, 1 H, Ar-H), 7.75−7.80 (m, 3 H, Ar-H). ^{13}C NMR (100 MHz, $CDCl_3$): δ [ppm] = 18.5 (q), 24.8 (t), 25.9 (t), 32.4 (t), 34.2 (t), 49.8 (d), 75.6 (d), 119.1 (d), 125.1 (d), 125.7 (d), 125.9 (d), 126.0 (d), 127.5 (d), 127.6 (d), 127.8 (d), 129.7 (d), 132.4 (s), 133.5 (s), 138.7 (d), 140.8 (s), 144.5 (d), 166.5 (s). $C_{22}H_{24}O_2$ (320.4): calcd. C 82.46, H 7.55; found C 82.21, H 7.56.

PTAD Adducts: The diastereomeric ratios of the crude products are given in Table 2 and Scheme 2, the yields were quantitative in all cases.

Representative Procedure for 2-[1-Methyl-1-(2-naphthyl)ethyl]-cyclohexyl 8-Methyl-1,3-dioxo-2-phenyl-2,3,5,8-tetrahydro-1*H*-[1,2,4]triazolo[1,2-*a*]pyridazine-5-carboxylate (6F): To a solution of ester **2F** (460 mg, 1.27 mmol) in 5 mL of CH_2Cl_2 at 0 °C, was added solid PTAD (222 mg, 1.27 mmol) in small portions with a glass spatula. After 10 min of stirring, the solvent was evaporated (20 °C, 20 mbar), a ^{1}H NMR spectrum was recorded and the two diastereomers were separated by silica gel chromatography [PE/Et_2O (6:1)] and 500 mg (73%) of the pure major isomer as well as 170 mg (25%) of the pure minor isomer (total yield 98%) were isolated. Recrystallization of the major isomer from Et_2O afforded colorless cubes, which were submitted to X-ray analysis (see Figure 1); m.p. 144−145 °C. IR (KBr): ṽ [cm^{-1}] = 2934, 1779, 1719, 1503, 1419, 1210. $C_{33}H_{35}N_3O_4$ (537.7): calcd. C 73.72, H 6.56, N 7.82; found C 73.66, H 6.70, N 7.66. **Major Isomer:** ^{1}H NMR (400 MHz, $CDCl_3$): δ [ppm] = 1.02−1.47 (m, 4 H, CH_2), 1.30 (s, 3 H, CH_3), 1.43 (s, 3 H, CH_3), 1.53−1.77 (m, 3 H, CH_2), 1.59 (d, J = 6.8 Hz, 3 H, CH_3), 1.99−2.08 (m, 1 H, CH_2), 2.24−2.31 (m, 1 H, CH), 4.22−4.29 (m, 1 H, CH), 4.66−4.69 (m, 1 H, CH), 4.96−5.05 (m, 2 H, CH), 5.21 (ddd, J = 10.4, 2.3, 2.3 Hz, 1 H, CH), 7.34−7.38 (m, 1 H, Ar-H), 7.42−7.49 (m, 2 H, Ar-H), 7.50−7.55 (m, 3 H, Ar-H), 7.65 (br. s, 1 H, Ar-H), 7.77−7.84 (m, 3 H, Ar-H). ^{13}C NMR (100 MHz, $CDCl_3$): δ [ppm] = 19.5 (q), 24.4 (t), 25.6 (t), 26.6 (q), 27.0 (q), 27.2 (t), 33.3 (t), 40.3 (s), 49.5 (d), 51.6 (d), 55.6 (d), 78.0 (d), 117.1 (d), 123.1 (d), 124.9 (d), 125.3 (d), 125.7 (d), 125.9 (d), 127.3 (d), 127.5 (d), 128.1 (d), 129.0 (2 × d), 129.7 (d), 131.2 (s), 131.6 (s), 133.6 (s), 148.5 (s), 152.0 (s), 152.6 (s), 166.3 (s). **Minor Isomer:** ^{1}H NMR (400 MHz, $CDCl_3$): δ [ppm] = 1.06−1.39 (m, 4 H, CH_2), 1.32 (s, CH_3), 1.44 (s, 3 H, CH_3), 1.55 (d, J = 6.7 Hz, 3 H, CH_3), 1.66−1.74 (m, 2 H, CH_2), 1.82−1.87 (m, 1 H, CH_2), 1.90−1.94 (m, 1 H, CH_2), 2.20−2.30 (m, 1 H, CH), 4.00−4.03 (m, 1 H, CH), 4.19−4.28 (m, 1 H, CH), 4.83−4.90 (m, 1 H, CH), 5.21 (ddd, J = 10.1, 5.2, 2.1 Hz, 1 H, CH), 5.54 (ddd, J = 10.1, 2.1, 2.1 Hz, 1 H, CH), 7.36−7.59 (m, 8 H, Ar-H), 7.73−7.91 (m, 4 H, Ar-H). ^{13}C NMR (100 MHz, $CDCl_3$): δ [ppm] = 19.4 (q), 24.2 (q), 24.5 (t), 25.8 (t), 26.9 (t), 28.2 (q), 33.0 (t), 39.9 (s), 50.7 (d), 51.7 (d), 55.0 (d), 77.4 (d), 117.9 (d), 123.0 (d), 124.9 (d), 125.3 (d), 125.8 (d), 125.9 (d), 127.1 (d), 127.4 (d), 128.1 (d), 129.1 (2 × d), 129.8 (d), 131.3 (s), 131.4 (s), 133.3 (s), 149.3 (s), 152.1 (s), 152.8 (s), 165.9 (s).

2-[1-Methyl-1-(4-phenoxyphenyl)ethyl]cyclohexyl 8-Methyl-1,3-dioxo-2-phenyl-2,3,5,8-tetrahydro-1*H*-[1,2,4]triazolo[1,2-*a*]pyridazine-5-carboxylate (6D): According to the method described for **6F**, the PTAD adduct **6D** was obtained quantitatively as a white powder, m.p. 166−168 °C. IR (KBr): ṽ [cm^{-1}] = 2931, 1774, 1718, 1504, 1487, 1418, 1241, 1201. $C_{35}H_{37}N_3O_5$ (579.7): calcd. C 75.52, H 6.43, N 7.25; found C 72.22, H 5.95, N 6.87. **Major Isomer:** ^{1}H NMR (400 MHz, $CDCl_3$): δ [ppm] = 0.98−1.44 (m, 4 H, CH_2), 1.28 (s, 3 H, CH_3), 1.35 (s, 3 H, CH_3), 1.54−1.72 (m, 3 H,CH_2), 1.65 (d, J = 6.7 Hz, 3 H, CH_3), 2.03−2.08 (m, 1 H, CH_2), 2.13 (m, 1 H, CH), 4.35−4.41 (m, 1 H, CH), 4.82−4.84 (m, 1 H, CH), 4.95 (ddd, J = 4.3, 10.1, 10.1 Hz, 1 H, CH), 5.58 (ddd, J = 2.0, 5.0, 10.2 Hz, 1 H, CH), 5.73 (ddd, J = 2.3, 2.3, 10.2 Hz, 1 H, CH), 7.31−7.39 (m, 4 H, Ar-H), 7.41−7.49 (m, 4 H, Ar-H), 7.52−7.56 (m, 4 H, Ar-H), 7.59−7.63 (m, 2 H, Ar-H). ^{13}C NMR (100 MHz, $CDCl_3$): δ [ppm] = 19.4 (q), 24.4 (t), 25.6 (t), 26.2 (q), 27.2 (t), 27.8 (q), 33.2 (t), 40.1 (s), 50.0 (d), 51.7 (d), 55.7 (d), 78.1 (d), 117.6 (d), 125.7 (d), 126.1 (d), 126.7 (d), 126.8 (d), 127.1 (d), 128.1 (d), 128.8 (d), 129.1 (d), 130.2 (d), 131.2 (s), 138.1 (s), 140.7 (s), 149.8 (s), 152.1 (s), 152.6 (s), 166.3 (s). **Minor Isomer:** ^{1}H NMR (400 MHz, $CDCl_3$): δ [ppm] = 1.09−1.40 (m, 6 H, CH_2), 1.26 (s, 3 H, CH_3), 1.35 (s, 3 H, CH_3), 1.58 (d, J = 6.6 Hz, 3 H, CH_3), 1.68−1.77 (m, 2 H, CH_2), 1.88−1.96 (m, 2 H, CH_2), 2.13−2.19 (m, 1 H, CH), 4.22−4.32 (m, 2 H, CH), 4.78−4.85 (m, 1 H, CH), 5.41−5.46 (m, 1 H, CH), 5.59−5.63 (m, 1 H, CH), 7.31−7.51 (m, 9 H, Ar-H), 7.54−7.63 (m, 6 H, Ar-H). ^{13}C NMR (100 MHz, $CDCl_3$): δ [ppm] = 19.6 (q), 23.2 (q), 24.5 (t), 25.8 (t), 26.7 (t), 29.1 (q), 33.0 (t), 39.4 (s), 50.9 (d), 51.9 (d), 55.0 (d), 77.1 (d), 118.2 (d), 125.8 (d), 125.9 (d), 126.7 (d), 126.9 (d), 127.0 (d), 128.1 (d), 128.7 (d), 129.1 (d), 129.9 (d), 131.3 (s), 137.8 (s), 140.9 (s), 151.2 (s), 152.0 (s), 153.0 (s), 165.8 (s).

2-[1-Methyl-1-(4-phenylphenyl)ethyl]cyclohexyl 8-Methyl-1,3-dioxo-2-phenyl-2,3,5,8-tetrahydro-1*H*-[1,2,4]triazolo[1,2-*a*]pyridazine-5-carboxylate (6E): According to the method described for **6F**, the PTAD adduct **6E** was obtained quantitatively as a white powder, m.p. 190−191 °C. IR (KBr): ṽ [cm^{-1}] = 2973, 2932, 2855, 1773, 1715, 1503, 1489, 1418, 1219, 1143, 1121. $C_{18}H_{15}O$ (563.7) HRMS (EI), $[M]^+$: calcd: 563.2784, found 563.2785. **Major Isomer:** ^{1}H NMR (400 MHz, $CDCl_3$): δ [ppm] = 0.96−1.44 (m, 4 H, CH_2), 1.28 (s, 3 H, CH_3), 1.36 (s, 3 H, CH_3), 1.56−1.70 (m, 3 H, CH_2), 1.65 (d, J = 6.0 Hz, 3 H, CH_3), 2.02−2.09 (m, 1 H, CH_2), 2.10−2.17 (m, 1 H, CH), 4.35−4.41 (m, 1 H, CH), 4.82−8.84 (m, 1 H, CH), 4.96 (td, J = 4.4, 10.2 Hz, 1 H, CH), 5.58 (ddd, J = 10.2, 5.0, 2.0 Hz, 1 H, H3), 5.73 (ddd, J = 10.2, 2.2, 2.2 Hz, 1 H, CH), 7.32−7.40 (m, 4 H, Ar-H), 7.42−7.48 (m, 4 H, Ar-H), 7.53−7.56 (m, 4 H, Ar-H), 7.59−7.62 (m, 2 H, Ar-H). ^{13}C NMR (100 MHz, $CDCl_3$): δ [ppm] = 19.43 (q), 24.4 (d), 25.6 (d), 26.2 (q), 27.2 (d), 27.8 (q), 33.2 (d), 40.1 (s), 50.0 (d), 51.7 (d), 55.7 (d), 78.1 (d), 117.6 (d), 125.7 (d), 126.1 (d), 126.7 (d), 126.8 (d), 127.1 (d), 128.1 (d), 128.8 (d), 129.1 (d), 130.2 (d), 131.2 (s), 138.1 (s), 140.7 (s), 149.8 (s), 152.1 (s), 152.6 (s), 166.3 (s). **Minor Isomer:** ^{1}H NMR (400 MHz, $CDCl_3$): δ [ppm] = 1.09−1.36 (m, 4 H, CH_2), 1.26 (s, 3 H, CH_3), 1.35 (s, 3 H, CH_3), 1.58 (d, J = 6.6 Hz, 3 H, CH_3), 1.67−1.78 (m, 2 H, CH_2), 1.88−1.96 (m, 2 H, CH_2), 2.12−2.19 (m, 1 H, CH), 4.22−4.31 (m, 2 H, CH), 4.77−4.86 (m, 1 H, CH), 5.43 (ddd, J = 10.1, 5.2, 2.0 Hz, 1 H, CH), 5.58−5.64 (m, 1 H, CH),

7.30−7.49 (m, 10 H, Ar-H), 7.53−7.62 (m, 4 H, Ar-H). ^{13}C NMR (100 MHz, $CDCl_3$): δ [ppm] = 19.6 (q), 23.3 (q), 24.6 (t), 25.9 (t), 26.7 (t), 29.1 (q), 33.0 (t), 39.9 (s), 51.0 (d), 51.9 (d), 55.1 (d), 77.2 (d), 118.2 (d), 125.9 (d), 126.0 (d), 126.8 (d), 126.9 (d), 127.0 (d), 128.1 (d), 128.7 (d), 129.1 (d), 129.9 (d), 131.3 (s), 137.9 (s), 141.0 (s), 151.2 (s), 152.1 (s), 153.0 (s), 165.9 (s).

2-Phenylcyclohexyl 8-Methyl-1,3-dioxo-2-phenyl-2,3,5,8-tetrahydro-1*H*-[1,2,4]triazolo[1,2-*a*]pyridazine-5-carboxylate (6G): According to the method described for **6F**, the PTAD adduct **6G** was obtained quantitatively as a white powder, m.p. 148−149 °C. The two diastereomers could not be separated by silica gel chromatography [PE/Et_2O (5:1)]. IR (KBr): $\tilde{\nu}$ [cm^{-1}] = 2933, 2876, 1778, 1740, 1716, 1503, 1418, 1213, 1156, 1123, 1009. $C_{26}H_{27}N_3O_4$ (445.5): calcd. C 70.10, H 6.11, N 9.43, found C 69.57, H 5.72, N 9.74. **Major Isomer:** ^{1}H NMR (400 MHz, $CDCl_3$): δ [ppm] = 1.28−1.67 (m, 4 H, CH_2), 1.47 (d, 6.7 Hz, 3 H, CH_3), 1.78−2.02 (m, 4 H, CH_2), 2.20−2.26 (m, 1 H, CH), 2.70 (ddd, *J* = 3.6, 3.6, 11.1 Hz, 1 H, CH), 4.24−4.32 (m, 1 H, CH), 4.82−4.86 (m, 1 H, CH), 5.05−5.13 (m, 1 H, CH), 5.30 (ddd, *J* = 2.0, 5.0, 10.1 Hz, 1 H, CH), 7.13−7.23 (m, 3 H, Ar-H), 7.25−7.31 (m, 2 H, Ar-H), 7.35−7.41 (m, 1 H, Ar-H), 7.45−7.55 (m, 4 H, Ar-H). ^{13}C NMR (100 MHz, $CDCl_3$): δ [ppm] = 19.5 (q), 24.7 (t), 25.6 (t), 32.3 (t), 34.0 (t), 50.2 (d), 51.4 (d), 78.6 (d), 117.4 (d), 125.7 (d), 126.5 (d), 127.5 (d), 128.0 (d), 128.4 (d), 128.5 (d), 129.0 (d), 129.5, 131.2 (s), 142.7 (s), 152.0 (s), 152.4 (s), 166.1 (s). **Minor Isomer:** ^{1}H NMR (600 MHz, $CDCl_3$): δ [ppm] = 1.40 (d, *J* = 6.7 Hz, 3 H, CH_3), 5.63 (ddd, *J* = 2.3, 2.3, 10.2 Hz, 1 H, CH), 5.77 (ddd, *J* = 2.2, 2.2, 10.2 Hz, 1 H, CH), the remaining signals overlap with those of the major isomer. ^{13}C NMR (100 MHz, $CDCl_3$): δ [ppm] = 19.2 (q), 24.5 (t), 25.6 (t), 32.0 (t), 34.4 (t), 49.6 (d), 51.6 (d), 55.1 (d), 77.3 (d), 118.1 (d), 125.4 (d), 126.5 (d), 127.2 (d), 128.0 (d), 128.5 (d), 129.1 (d), 129.9 (d), 131.3 (s), 142.4 (s), 151.7 (s), 152.5 (s), 166.3 (s).

2-(2-Naphthyl)cyclohexyl 8-Methyl-1,3-dioxo-2-phenyl-2,3,5,8-tetrahydro-1*H*-[1,2,4]triazolo[1,2-*a*]pyridazine-5-carboxylate (6H): According to the method described for **6F**, the PTAD adduct **6H** was obtained quantitatively as a white powder. The diastereomers could not be separated by silica gel chromatography [PE/Et_2O (6:1)], however, recrystallization from Et_2O/PE afforded a few crystals of the major isomer as colorless cubes, m.p. 159−164 °C, which were submitted to X-ray analysis (see Figure 1). IR (KBr): $\tilde{\nu}$ [cm^{-1}] = 2934, 3361, 1778, 1718, 1502, 1419, 1205, 1122, 1012. $C_{30}H_{29}N_3O_4$ (495.6): calcd. C 72.71, H 5.90, N 8.48, found C 72.47, H 6.03, N 8.46. **Major Isomer:** ^{1}H NMR (400 MHz, $CDCl_3$): δ [ppm] = 1.02 (d, *J* = 6.70 Hz, 3 H, CH_3), 1.35−1.49 (m, 1 H, CH_2), 1.51−1.61 (m, 2 H, CH_2), 1.63−1.74 (m, 1 H, CH_2), 1.80−1.87 (m, 1 H, CH_2), 1.90−1.95 (m, 1 H, CH_2), 2.01- 2.17 (m, 1 H, CH_2), 2.19−2.24 (m, 1 H, CH_2), 2.82−2.89 (m, 1 H, CH), 4.08−4.04 (m, 1 H, CH), 4.70 (dt, *J* = 10.2, 2.3 Hz, 1 H, CH), 4.74−4.77 (m, 1 H, CH), 5.11 (ddd, *J* = 10.2, 5.23, 2.2 Hz, 1 H, CH), 5.15−5.23 (m, 1 H, CH), 7.31−7.48 (m, 2 H, Ar-H), 7.40−7.48 (m, 6 H, Ar-H), 7.59 (br.s, 1 H, Ar-H), 7.75−7.79 (m, 3 H, Ar-H). ^{13}C NMR (100 MHz, $CDCl_3$): δ [ppm] = 18.9 (q), 24.8 (t), 25.7 (t), 32.3 (t), 33.7 (t), 50.6 (d), 51.1 (d), 54.7(d), 78.5 (d), 117.1 (d), 125.4 (d), 125.6 (d), 125.7 (d), 126.0 (d), 126.6 (d), 127.5 (d), 127.6 (d), 128.0 (d), 128.2 (d), 128.96 (d), 129.00 (d), 131.3 (s), 132.6 (s), 133.5 (s), 140.0 (s), 151.9 (s), 152.2 (s), 166.0 (s). **Minor Isomer:** ^{1}H NMR (400 MHz, $CDCl_3$): δ [ppm] = 1.11 (d, *J* = 6.72 Hz, CH_3), 4.15−4.20 (m, 1 H, CH), 5.42 (ddd, *J* = 2.3, 2.3, 10.3 Hz, 1 H, CH), 5.62 (ddd, *J* =2.2, 4.9, 10.2 Hz, 1 H, CH), the remaining signals overlap with those of the major isomer. ^{13}C NMR (150 MHz, $CDCl_3$): δ [ppm] = 18.7 (q), 24.6 (t), 25.7 (t), 32.0 (t), 34.5 (t), 49.8 (d), 51.4 (d), 55.1 (d), 78.1 (d), 117.9 (d), 125.3 (d), 125.8 (d), 125.9 (d), 126.6 (d), 127.4 (d), 127.7 (d), 128.0 (d), 128.2 (d), 128.9 (d), 129.1 (d), 129.8 (d), 131.3 (s), 132.5 (s), 133.5 (s), 139.9 (s), 151.7 (s), 152.4 (s), 166.4 (s).

(1*S*,2*R*)-Bornane-10,2-sultam Derivative 6I: According to the method described for **6F**, the PTAD adduct **6I** was obtained quantitatively as a white amorphous solid. The isolated major isomer could not be crystallized; however, the minor isomer crystallized from acetone as pale yellow cubes, m.p. 214−215 °C, and was submitted to X-ray analysis (see Figure 1). IR (KBr): $\tilde{\nu}$ [cm^{-1}] = 2949, 1771, 1706, 1598, 1412, 1333, 1315, 1289, 1219, 1134. $C_{24}H_{28}N_4O_5S$ (484.6): calcd. C 59.49, H 5.82, N 11.56, 6.62; found C 59.07, H 5.41, N 11.08, S 6.60. **Major Isomer:** ^{1}H NMR (400 MHz, $CDCl_3$): δ [ppm] = 0.96 (s, 3 H, CH_3), 1.22 (s, 3 H, CH_3), 1.30−1.45 (m, 2 H, CH_2), 1.60 (d, *J* = 6.8 Hz, 3 H, CH_3), 1.85−1.97 (m, 3 H, CH, CH_2), 2.01 (dd, *J* = 7.9, 14.0 Hz, 1 H, CH_2), 2.27−2.34 (m, 1 H, CH_2), 3.47 (d, *J* = 13.6 Hz, 1 H, CH_2), 3.56 (d, *J* = 13.6 Hz, 1 H, CH_2), 3.91 (dd, *J* = 5.0, 7.8 Hz, 1 H, CH), 4.49−4.53 (m, 1H, CH), 5.60−5.62 (m, 1 H, CH), 6.02 (ddd, *J* = 2.2, 3.6, 10.4 Hz, 1 H, CH), 6.18 (ddd, *J* = 1.8, 3.6, 10.4 Hz, 1 H, CH), 7.32−7.36 (m, 1H, Ar-H), 7.42−7.46 (m, 2 H, Ar-H), 7.49−7.53 (m, 2 H, Ar-H). ^{13}C NMR (100 MHz, $CDCl_3$): δ [ppm] = 18.6 (q), 19.9 (q), 20.5 (q), 26.5 (t), 32.6 (t), 37.7 (t), 44.3 (d), 48.0 (s), 49.4 (s), 50.1 (d), 52.9 (t), 56.2 (d), 65.6 (d), 117.5 (d), 125.6 (d), 128.0 (d), 129.1 (d), 130.1 (d), 131.1 (s), 151.1(s), 151.8 (s), 165.8 (s). $[\alpha]_D^{20} = -13.0$ (*c* = 1.0, $CHCl_3$). **Minor Isomer:** ^{1}H NMR (400 MHz, $CDCl_3$): δ [ppm] = 0.95 (s, 3 H, CH_3), 1.23 (s, 3 H, CH_3), 1.31−1.42 (m 2 H, CH_2), 1.66 (d, *J* = 6.7 Hz, 3 H, CH_3), 1.82−1.94 (m, 3 H, CH_2), 1.96−2.09 (m, 2 H, CH_2), 3.42−3.63 (m, 2 H, CH_2), 3.94−3.97 (m, 1 H, CH), 4.40−4.47 (m, 1 H, CH), 5.60−6.63 (m, 1 H, CH), 5.89 (dt, *J* = 10.3, 2.4 Hz, 1 H, CH), 6.17 (ddd, *J* = 2.0, 4.8, 10.3 Hz, CH), 7.30−7.45 (m, 1 H, Ar-H), 7.39−7.44 (m, 2 H, Ar-H), 7.53−7.55 (m, 2 H, Ar-H). ^{13}C NMR (100 MHz, $CDCl_3$): δ [ppm] = 19.3 (q), 19.7 (q), 20.7 (q), 26.3 (t), 32.5 (t), 37.7 (t), 44.5 (d), 47.8 (s), 48.9 (s), 51.2 (d), 52.7 (t), 56.5 (d), 65.1 (d), 117.6 (d), 125.5 (d), 127.8 (d), 128.8 (d), 131.22 (s), 131.24 (d), 151.7 (s), 152.0 (s), 165.8 (s).

Endoperoxides

General Procedure for the Photo-Oxygenation of Sorbates 2: A solution of the particular ester **2** (30−60 mg) and ca. 2 mg of tetrakis(perfluorophenyl)porphine in 5 mL of CCl_4 was irradiated with two external Osram Violax NAV-T 400-W sodium lamps at −5 °C, while a stream of dry oxygen gas was allowed to pass continuously through the reaction mixture. After 16 h, the solvent was evaporated (20 °C, 20 mbar) and the composition of the crude reaction mixture was determined by ^{1}H and ^{13}C NMR spectroscopy (for the product ratios of the endoperoxides **5**, cf. Table 2 and Scheme 2). The labile endoperoxides **5** could not be isolated and were characterized only by their ^{1}H and ^{13}C NMR resonances directly in the crude reaction mixtures.

2-[1-Methyl-1-(4-phenoxyphenyl)ethyl]cyclohexyl 6-Methyl-3,6-dihydro-1,2-dioxine-3-carboxylate (5D): Major Isomer: ^{1}H NMR (600 MHz, $CDCl_3$): δ [ppm] = 0.97−1.42 (m, 4 H, CH_2), 1.14 (d, *J* = 4.6 Hz, 3 H, CH_3), 1.25 (s, 3 H, CH_3), 1.33 (s, 3 H, CH_3), 1.57−1.86 (m, 3 H, CH_2), 1.92−1.96 (m, 1 H, CH_2), 2.04−2.12 (m, 1 H, CH), 4.39 (ddd, *J* = 4.1, 2.0, 2.0 Hz, 1 H, CH), 4.75−4.83 (m, 1 H, CH), 4.93 (ddd, *J* = 10.5, 10.5, 4.6 Hz, 1 H, CH), 5.59 (ddd, *J* = 10.2, 4.4, 2.2 Hz, 1 H, CH), 5.94 (ddd, *J* = 10.2, 1.8, 1.3 Hz, 1 H, CH), 6.91−6.93 (m, 2 H, Ar-H), 6.96−7.02 (m, 2 H, Ar-H), 7.06−7.10 (m, 1 H, Ar-H), 7.23−7.26 (m, 2 H, Ar-H), 7.29−7.33 (m, 2 H, Ar-H). ^{13}C NMR (150 MHz, $CDCl_3$): δ [ppm] = 17.1, 24.6, 25.7, 26.2, 26.8, 27.2, 33.2, 40.0, 50.5, 74.1, 75.9, 76.4, 121.6, 126.1, 126.6, 126.9, 127.0, 128.7, 130.7, 138.0, 140.9, 150.0, 167.9.

Minor Isomer: ^{1}H NMR (600 MHz, $CDCl_3$): δ [ppm] = 1.13 (d, J = 4.9 Hz, 3 H, CH_3), 1.21 (s, 3 H, CH_3), 1.32 (s, 3 H, CH_3), 4.15 (ddd, J = 4.5, 2.3, 2.3 Hz, 1 H, CH), 4.84−4.89 (m, 1 H, CH), 5.87 (ddd, J = 10.2, 2.3, 1.5 Hz, 1 H, CH), 5.98 (ddd, J = 10.2, 4.2, 2.1 Hz, 1 H, CH), the remaining signals overlap with those of the major isomer. ^{13}C NMR (150 MHz, $CDCl_3$): δ [ppm] = 17.3, 24.8, 25.9, 26.1, 26.7, 27.2, 33.2, 39.5, 50.8, 73.8, 75.6, 76.1, 121.5, 125.8, 126.6, 126.9, 127.0, 128.7, 130.3, 138.0, 140.9, 151.2, 167.4.

2-[1-Methyl-1-(4-phenylphenyl)ethyl]cyclohexyl 6-Methyl-3,6-dihydro-1,2-dioxine-3-carboxylate (5E): Major Isomer: ^{1}H NMR (600 MHz, $CDCl_3$): δ [ppm] = 1.03−1.45 (m, 4 H, CH_2), 1.13 (d, J = 6.8 Hz, 3 H, CH_3), 1.30 (s, 3 H, CH_3), 1.38 (s, 3 H, CH_3), 1.61−1.78 (m, 3 H, CH_2), 1.91−1.99 (m, 1 H, CH_2), 2.14−2.21 (m, 1 H, CH), 4.27−4.30 (m, 1 H, CH), 4.74−4.79 (m, 1 H, CH), 4.98 (ddd, J = 4.7, 10.5, 10.5 Hz, 1 H, CH), 5.88 (ddd, J = 1.3, 1.6, 10.2 Hz, 1 H, CH), 5.92 (ddd, J = 2.0, 4.2, 10.2 Hz, 1 H, CH), 7.31−7.35 (m, 1 H, Ar-H), 7.37−7.45 (m, 4 H, Ar-H), 7.51−7.60 (m, 4 H, Ar-H). ^{13}C NMR (150 MHz, $CDCl_3$): δ [ppm] = 17.0, 24.6, 25.7, 26.6, 26.8, 29.5, 33.2, 40.0, 50.5, 74.1, 75.9, 76.4, 121.6, 126.1, 126.6, 126.9, 127.0, 128.7, 130.7, 138.0, 140.9, 150.0, 167.9. **Minor Isomer:** ^{1}H NMR (600 MHz, $CDCl_3$): δ [ppm] = 1.09 (d, J = 6.8 Hz, 3 H, CH_3), 1.25 (s, 3 H, CH_3), 1.37 (s, 3 H, CH_3), 3.97−3.99 (m, 1 H, CH), 4.68−4.73 (m, 1 H, CH), 4.88−4.92 (m, 1 H, CH), 5.39 (ddd, J = 2.2, 4.5, 10.2 Hz, 1 H, CH), 5.74 (ddd, J = 1.6, 2.2, 10.2 Hz, 1 H, CH), the remaining signals overlap with those of the major isomer. ^{13}C NMR (150 MHz, $CDCl_3$): δ [ppm] = 17.0, 23.0, 25.9, 26.7, 27.2, 29.5, 33.2, 39.5, 50.8, 73.8, 75.6, 76.1, 121.5, 125.8, 126.6, 126.9, 127.0, 128.7, 130.3, 138.0, 140.9, 151.2, 167.4.

2-[1-Methyl-1-(2-naphthyl)ethyl]cyclohexyl 6-Methyl-3,6-dihydro-1,2-dioxine-3-carboxylate (5F): Major Isomer: ^{1}H NMR (600 MHz, $CDCl_3$): δ [ppm] = 1.08 (d, J = 7.0 Hz, 3 H, CH_3), 1.34 (s, 3 H, CH_3), 1.44 (s, 3 H, CH_3), 1.05−1.44 (m, 4 H, CH_2), 1.58−1.74 (m, CH_2), 1.90−1.97 (m, 1 H, CH_2), 2.21−2.27 (m, 1 H, CH), 3.96 (ddd, J = 4.3, 2.1, 2.1 Hz, 1 H, CH), 4.66−4.70 (m, 1 H, CH), 5.00 (ddd, J = 10.4, 10.4, 4.6 Hz, 1 H, CH), 5.54 (ddd, J = 10.2, 4.4, 2.1 Hz, 1 H, CH), 5.62−5.65 (m, 1 H, CH), 7.39−7.45 (m, 2 H, Ar-H), 7.51−7.55 (m, 1 H, Ar-H), 7.63 (d, J = 1.7 Hz, Ar-H), 7.75−7.80 (m, 3 H, Ar-H). ^{13}C NMR (150 MHz, $CDCl_3$): δ [ppm] = 17.5, 25.1, 26.2, 26.8, 27.3, 27.6, 33.7 40.7, 50.5, 74.4, 76.2, 76.7, 121.7, 123.2, 125.6, 125.7, 126.3, 127.8, 127.9, 128.3, 130.9, 131.9, 133.8, 149.0, 168.2. **Minor Isomer:** ^{1}H NMR (600 MHz, $CDCl_3$): δ [ppm] = 1.04 (d, J = 7.0 Hz, 3 H, CH_3), 1.30 (s, 3 H, CH_3), 1.83−1.87 (m, 1 H, CH_2), 3.63 (ddd, J = 4.4, 2.1, 2.1 Hz, 1 H, CH), 4.60−4.64 (m, 1 H, CH), 4.94 (ddd, J = 10.5, 10.5, 4.6 Hz, 1 H, CH), 5.16 (ddd, J = 10.2, 4.5, 2.2 Hz, 1 H, CH), 7.64 (d, J = 1.8 Hz, 1 H, Ar-H), the remaining signals overlap with those of the major isomer. ^{13}C NMR (150 MHz, $CDCl_3$): δ [ppm] = 17.5, 25.1, 26.3, 26.8, 27.3, 27.6, 33.7, 40.4, 50.9, 74.2, 76.2, 76.4, 121.8, 123.0, 125.4, 125.8, 126.5, 127.6, 127.7, 128.2, 130.5, 131.8, 133.7, 149.8, 167.9.

2-Phenylcyclohexyl 6-Methyl-3,6-dihydro-1,2-dioxine-3-carboxylate (5G): Major Isomer: ^{1}H NMR (600 MHz, $CDCl_3$): δ [ppm] = 1.01 (d, J = 7.0 Hz, 3 H, CH_3), 1.24−1.60 (m, 5 H, CH_2), 1.69−1.91 (m, 3 H, CH_2), 2.06−2.12 (m, 1 H, CH_2), 2.68−2.75 (m, 1 H, CH), 4.59 (ddd, J = 4.4, 2.2, 2.2 Hz, 1 H, CH), 4.65−4.72 (m, 1 H, CH), 5.05−5.11 (m, 1 H, CH), 5.56 (ddd, J = 10.3, 4.1, 2.1 Hz, 1 H, CH), 5.65 (ddd, J = 10.2, 2.2, 1.6 Hz, 1 H, CH), 7.13−7.20 (m, 3 H, Ar-H), 7.21−7.25 (m, 2 H, Ar-H). ^{13}C NMR (150 MHz, $CDCl_3$): δ [ppm] = 17.1, 24.6, 25.7, 33.1, 33.8, 49.9, 73.8, 76.0, 77.2, 121.2, 126.3, 127.5, 128.2, 130.2, 142.7, 167.7. **Minor Isomer:** ^{1}H NMR (600 MHz, $CDCl_3$): δ [ppm] = 1.06 (d, J = 6.8 Hz, 3 H, CH_3), 4.51 (ddd, J = 4.3, 2.2, 2.2 Hz, 1 H, CH), 5.85 (ddd, J = 10.1, 2.1, 1.4 Hz, 1 H, CH), 5.91 (ddd, J = 10.1, 4.1, 2.0 Hz, 1 H, CH), the remaining signals overlap with those of the major isomer. ^{13}C NMR (150 MHz, $CDCl_3$): δ [ppm] = 17.0, 24.6, 25.7, 32.1, 33.8, 49.9, 73.8, 76.0, 77.2, 121.5, 126.4, 127.4, 128.2, 130.7, 142.6, 167.5.

2-(2-Naphthyl)cylcohexyl 6-Methyl-3,6-dihydro-1,2-dioxine-3-carboxylate (5H): Major Isomer: ^{1}H NMR (600 MHz, $CDCl_3$): δ [ppm] = 0.65 (d, J = 6.9 Hz, 3 H, CH_3), 0.94−1.98, 2.18−2.24 (m, 8 H, CH_2), 2.86−2.95 (m, 1 H, CH_2), 4.52−4.54 (m, 1 H, CH), 4.58−4.63 (m, 1 H, CH), 5.18−5.24 (m, 1 H, CH), 5.25 (ddd, J = 10.2, 2.1, 1.4 Hz, 1 H, CH), 5.46 (ddd, J = 10.2, 4.1, 1.9 Hz, 1 H, CH), 7.34−7.55 (m, 2 H, Ar-H), 7.60 (d, J = 1.0 Hz, 1 H, Ar-H), 7.73−7.98 (m, 4 H, Ar-H). ^{13}C NMR (150 MHz, $CDCl_3$): δ [ppm] = 16.5, 24.7, 25.7, 32.2, 33.6, 50.1, 73.4, 75.8, 77.1, 121.0, 125.2, 125.5, 126.4, 127.4, 127.5, 127.9, 129.9, 130.6, 132.4, 133.4, 140.1, 167.4. **Minor Isomer:** ^{1}H NMR (600 MHz, $CDCl_3$): δ [ppm] = 0.82 (d, J = 6.9 Hz, 1 H, CH_3), 4.47 (ddd, J = 4.4, 2.3, 2.3 Hz, 1 H, CH), 5.74 (ddd, J = 10.2, 2.2, 1.6 Hz, 1 H, CH), 5.85 (ddd, J = 10.1, 4.2, 2.1 Hz, 1 H, CH), 7.63 (d, J = 1.0 Hz, 1 H, Ar-H), the remaining signals overlap with those of the major isomer. ^{13}C NMR (150 MHz, $CDCl_3$): δ [ppm] = 16.7, 24.7, 25.7, 32.2, 34.0, 49.7, 73.6, 76.0, 77.1, 121.4, 125.2, 125.7, 126.4, 127.4, 127.6, 127.8, 129.9, 130.6, 132.4, 133.4, 140.2, 167.6.

(1*S*,2*R*)-Bornane-10,2-sultam Derivative 5I: Major Isomer: ^{1}H NMR (600 MHz, $CDCl_3$): δ [ppm] = 0.98 (s, 3 H, CH_3), 1.18 (d, J = 6.9 Hz, CH_3), 1.23 (s, 3 H, CH_3), 1.32−1.49 (m, 3 H, CH and CH_2), 1.86−1.95 (m, 2 H, CH_2), 2.20−2.14 (m, 2 H, CH_2), 3.41(d, J = 13.7 Hz, 1 H, CH_2), 3.53 (d, J = 13.7 Hz, 1 H, CH_2), 3.94−3.98 (m, 1 H, CH), 4.84−4.89 (m, 1 H, CH), 5.25−5.28 (m, 1 H, CH), 6.03 (ddd, J = 1.4, 1.4, 10.2 Hz, 1 H, CH), 6.08 (ddd, J = 1.9, 4.1, 10.2, Hz, 1 H, CH). ^{13}C NMR (50 MHz, $CDCl_3$): δ [ppm] = 16.7, 19.5, 20.9, 26.0, 32.8, 38.1, 44.8, 47.5, 48.5, 52.9, 65.6, 74.4, 77.3, 121.4, 131.7, 169.3. **Minor Isomer:** ^{1}H NMR (600 MHz, $CDCl_3$): δ [ppm] = 0.96 (s, 3 H, CH_3), 1.21 (d, J = 6.8 Hz, 3 H, CH_3), 1.12 (s, 3 H, CH_3), 3.44−3.49 (m, 1 H, CH_2), 4.76−4.81 (m, 1 H, CH), 5.39−5.41 (m, 1 H, CH), 6.20 (ddd, J = 2.0, 4.0, 10.2 Hz, 1 H, CH), the remaining signals overlap with those of the major isomer. ^{13}C NMR (50 MHz, $CDCl_3$): δ [ppm] = 16.8, 19.5, 20.3, 26.1, 32.3, 37.6, 44.2, 47.7, 48.7, 52.6, 65.0, 73.4, 76.4, 121.2, 132.8, 167.6.

X-ray Data: Crystal data for **6F**, **6H**, and **6I** were collected from shock-cooled crystals with a Bruker SMART-APEX diffractometer with D8 goniometer (graphite-monochromated Mo-K_α radiation, λ = 0.71073 Å), equipped with a low-temperature device in ω-scan mode at 193(2) K.[24] The data was integrated with SAINT[25] and an empirical absorption correction was applied.[26] The structures were solved by direct methods (SHELXS-97)[27] and refined by full-matrix least-squares methods against F^2 (SHELXL-97).[28] All non-hydrogen atoms were refined with anisotropic displacement parameters. All hydrogen atoms bonded to sp^3-carbon atoms were assigned ideal positions and refined using a riding model with U_{iso} constrained to 1.5 times the U_{eq} value of the parent atom and all hydrogen atoms bonded to sp^2-carbon atoms were assigned ideal positions and refined using a riding model with U_{iso} constrained to 1.2 times the U_{eq} value of the parent atom. Crystallographic data for the structures reported in this paper have been deposited with the Cambridge Crystallographic Data Centre as supplementary publication no. CCDC-185192 (**6F**), -185191 (**6H**), and -185193 (**6I**). Copies of the data can be obtained free of charge on application to CCDC, 12 Union Road, Cambridge CB2 1EZ, UK [Fax: (internat.) + 44-1223/336-033; E-mail: deposit@ccdc.cam.ac.uk].

Acknowledgments

We are grateful to the Fonds der Chemischen Industrie (doctoral fellowship 1998−2000 for H.-G. D.) for generous financial support.

[1] W. Adam, M. Güthlein, E.-M. Peters, K. Peters, T. Wirth, *J. Am. Chem. Soc.* **1998**, *120*, 4091−4093.
[2] W. Adam, T. Wirth, A. Pastor, K. Peters, *Eur. J. Org. Chem.* **1998**, 501−506.
[3] W. Adam, K. Peters, E.-M. Peters, S. B. Schambony, *J. Am. Chem. Soc.* **2000**, *122*, 7610−7611.
[4] W. Adam, K. Peters, E.-M. Peters, S. B. Schambony, *J. Am. Chem. Soc.* **2001**, *123*, 7228−7232.
[5] P. H. Dussault, K. R. Woller, M. C. Hillier, *Tetrahedron* **1994**, *50*, 8929−8940.
[6] W. Adam, H.-G. Brünker, B. Nestler, *Tetrahedron Lett.* **1991**, *32*, 1957−1960.
[7] W. Adam, A. Griesbeck, *Synthesis* **1986**, 1050−1052.
[8] S. Kanemasa, H. Suenaga, K. Onimura, *J. Org. Chem.* **1994**, *59*, 6949−6954.
[9] S. Kanemasa, M. Namura, S. Yoshinaga, H. Yamamoto, *Tetrahedron* **1995**, *51*, 10463−10476.
[10] B. Mezrhab, F. Dumas, J. d'Angelo, C. Riche, *J. Org. Chem.* **1994**, *59*, 500−503.
[11] F. Dumas, B. Merzhab, J. d'Angelo, *J. Org. Chem.* **1996**, *61*, 2293−2304.
[12] D. P. Curran, B.H. Kim, J. Daugherty, T. A. Heffner, *Tetrahedron Lett.* **1988**, *29*, 3555−3558.
[13] B. H. Kim, J. Y. Lee, K. Kim, D. Whang, *Tetrahedron: Asymmetry* **1991**, *2*, 27−30.
[14] W. Oppolzer, G. Poli, A. J. Kingma, C. Starkemann, G. Bernardinelli, *Helv. Chim. Acta* **1987**, *70*, 2201−2214.
[15] W. Oppholzer, J.-P. Barras, *Helv. Chim. Acta* **1987**, *70*, 1666−1669.
[16] W. Adam, O. Krebs, C. R. Saha-Möller, *J. Am. Chem. Soc.*, submitted.
[17] Although the stereochemical descriptors should refer to the π-face on the incipient stereogenic center (C-α for the [4+2] cycloaddition and C-β for the ene reaction), we have chosen the α-carbon atom as common reference site to facilitate the comparison between the two reaction modes.
[18] [18a] W. Adam, U. Hoch, C. R. Saha-Möller, P. Schreier, *Angew. Chem. Int. Ed. Engl.* **1993**, *32*, 1737−1739. [18b] W. Adam, R.T. Fell, U. Hoch, C. R. Saha-Möller, P. Schreier, *Tetrahedron: Asymmetry* **1995**, *6*, 1047−1050. [18c] U. Hoch, Dissertation, University of Würzburg, **1996**. [18d]S. E. Drewes, R. F. A. Hoole, *Synth. Commun.* **1985**, *15*, 1067-1074.
[19] W. Adam, M. Güthlein, E.-M. Peters, K. Peters, T. Wirth, *J. Am. Chem. Soc.* **1998**, *120*, 4091−4093.
[20] H. Kim, D. P. Curran, *Tetrahedron* **1993**, *49*, 293−318.
[21] F. Dumas, C. Frissigné, J. Langlet, C. Giessner-Prettre, *J. Org. Chem.* **1999**, *64*, 4725−4732.
[22] R. A. Izydore, J. J. Chapman, J. A. Mitchel, R. Cummings, G. T. Jones, *J. Chem. Soc., Perkin Trans. 2* **1988**, 1415−1422.
[23] M. Vandewalle, J. Van der Eycken, W. Oppholzer, C. Vullioud, *Tetrahedron* **1986**, *42*, 4035−4043.
[24] D. Stalke, *Chem. Soc. Rev.* **1998**, *27*, 171.
[25] Bruker-AXS Inc., *SAINT-NT*, Madison WI, **2000**.
[26] G. M. Sheldrick, *SADABS 2.0*, University of Göttingen, **2000**.
[27] G. M. Sheldrick, *Acta Crystallogr., Sect. A* **1990**, *46*, 467.
[28] G. M. Sheldrick, *SHELXL-97*, University of Göttingen, **1997**.

Received June 6, 2002
[O02300]